Wireless Personal Communications (2021) 118:3129–3143
https://doi.org/10.1007/s11277-021-08171-2

Nano-Sensor Modelling for Intra-Body Nano-Networks

Mustafa Alper Akkaş[1]

Accepted: 28 January 2021 / Published online: 11 February 2021

Abstract
In this work, the author has evaluated the propagation of electromagnetic waves inside the human tissue such as blood, skin and fat for single-path and multi-path layers according to nano sensor transmit power calculations. In particular, the propagation characteristics of the Intra-Body Nano-Network communication channel are calculated using a theoretical approach. The analysis in this paper provides an evaluation related to the path loss, bit error rate, signal to noise ratio and the channel capacity. The model is evaluated for each single-path effect and multi-path effect. The effects of human tissue for each blood, skin and fat for single-path effect and multi-path are included in the analysis. The model frequency range is chosen from 0.01 to 1.5 THz frequencies, which are ideal for designing nano sensors antennae and using THz range for communication. This paper will also guide other researchers who are working on the electromagnetic radiation performance of Intra-Body Nano-Network and Nano sensors designed at the THz range.

Keywords Intra-body nano-networks · Human tissue · Path loss · Nano-communication · Terahertz · Channel analysis

1 Introduction

Next generation wearable technologies, which is also supported with Internet of Things (IoT) and Nano-technology have to be in miniature size. Therefore, the designers need to work on higher frequencies such as 0.1–10 THz to reduce antenna size [1]. With the help of Nano-technology, nano-communication and THz waves, nano or micro size machines can communicate with each other [2, 3]. Since nano-technology was put forward in 1959, it has not only gained great attention in body-centric applications, but it has also gained great attention in many other fields [4]. Nano-technology, nano-networks and nano-communication will greatly affect human life and health. Nano-machines which are especially designed for the human body can be placed inside the body or surface-mounted on the body. With the help of these technologies, patient data can be sent to monitoring centers independent of the patient location [5].

✉ Mustafa Alper Akkaş
alperakkas@ibu.edu.tr

[1] Department of Computer Engineering, Bolu Abant Izzet Baysal University, 14280 Bolu, Turkey

One of the most important parts to achieve nano-technology is improving nano-machines without battery. Nano-machines are nano sized nodes which are used for communication, sensing, computation etc. [6]. In Intra-Body Nano-Networks, communication is done by nano-machines which function like nano-nodes [1]. The communication between nano-nodes in Intra-Body Nano-Networks is still an open issue and there are challenges to be solved [7]. So far, two communication methods have been used for Intra-Body Nano-Networks. These are Electromagnetic Communication (EMC) and Molecular Communication (MC). EMC communication uses EM waves for communication and transmission of information. MC systems are different from EMC, forming a new and interdisciplinary research area, which use the absence or presence of a selected type of molecule to digitally encode messages [8]. Molecules are used as a communication carrier in MC systems. MC is a new, open and interdisciplinary research area, and there are many challenges to be solved. These challenges are definition of MC channel model, characterization of MC mechanisms, development of its architectures and the networks protocols [9].

As shown in Fig. 1, the magnitude of the node needs to be in the nanometer size because the place where nano-nodes are placed is too small in biomedical applications. Nano nodes require THz antennas for their dimensions in EM communication. In THz band communication, phase shifting effects and path loss fluctuates according to the environment. Therefore electromagnetic (EM) waves need to communicate where phase shifting effects and path loss fluctuates are minimum. In EMC transmission distance between nodes can be increased by using the bandwidths where absorption and path loss is minimum.

We know that battery dependent machines are limited to use. This rule is also valid for nano-machines. That is why alternative energy methods should be developed like changing vibrational movement, mechanical movement or hydraulic energy into electrical energy. Another alternative energy method is charging batteries wirelessly but it's not easy to implement. Whence, nano-machines transmit power is very important and is covered in this paper [10, 11]. Part of this work was presented in [12] and an extended version of the article is given in this study.

In this paper, the author has carried out calculations of the Path Loss, bit error rate (BER), signal to noise ratio (SNR) and Channel Capacity effect based on the channel model

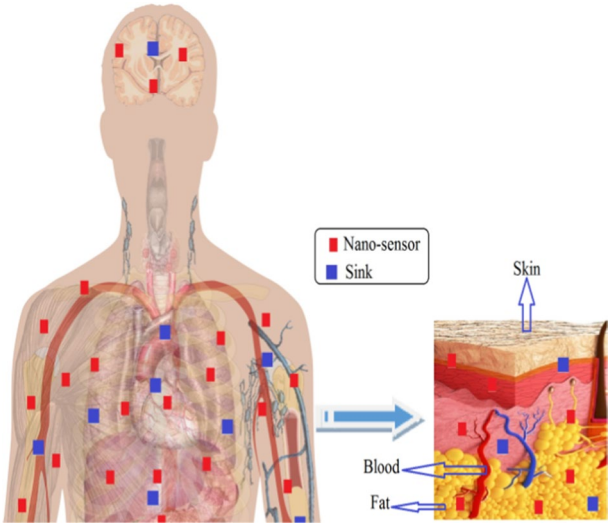

Fig. 1 A schematic network architecture for intra-body nano-networks with nano-sensors

for each single-path effect and multi-path effect, shown in Fig. 2. The effect of the human tissues according to Path Loss, BER, SNR and the Channel Capacity for each blood, skin and fat for single-path effect and multi-path effect are included in the all analysis.

This paper is organized as follows. In Sect. 2, related work is investigated. In Sect. 3, models for intra-body nano-networks for single and multi-layers are given. In Sect. 4, graphs of the theoretical model are shown. Conclusions are drawn in the last section.

2 Related Work

Akyıldız et al. [13] present an overview of two main alternatives for nano-communication, namely Electromagnetic Communication and Molecular Communication in the THz Band. The aim of the study is to provide a better understanding of current research topics in this important field and pave the way for future studies in nano-networks.

Yang et al. [14] modeled the human tissue with a 3-D numerical model at the THz range but they did not consider multi-layers according to the nano-sensor transmit power calculation. They also specify this lack in their conclusion part.

Pratap Singh et al. [8] analyzed the probability density function of radiation absorption noise and included the properties of different tissues of the human body to demonstrate its applicability. Also, the closed form expression of error probability for MNC under radiation noise is derived. Numerical analysis is shown in different tissues of the human body: The polarization factor of the incoming EM radiation is shown as well as the skin, brain and blood.

Again, Pratap Singh et al. [15] proposes a more general and appropriate noise model as the Gaussian distribution to derive a new closed form expression of the conditional error probability for the nano communication system. They have compared their noise model with different models in the literature. Finally, with respect to the conditional error probability, closed form statements derived for average bit error rate, the Weibull-Gamma and Mixture Gamma were derived from fading channels.

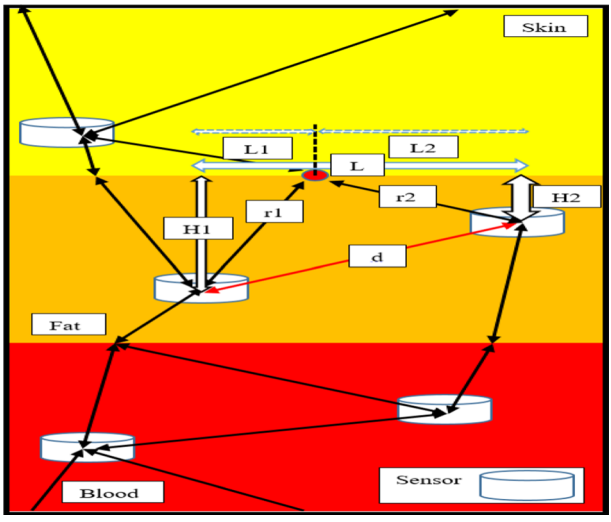

Fig. 2 Multi-path channel model

Hadeel Elayan et al. [16] analyzed the photo thermal effects of the THz range inside the human body as a heat diffusion mathematical model. Shortly they have analyzed EM waves release energy as a heat to their environment.

Zhang et al. [17] investigates the mathematical model for in vivo nano networks at the THz range including the information speed and the noise of link. In their analytical model, they have investigated signal-to-noise ratio according to different information and power allocation for body-centric nano-networks.

In their paper, Piro et al. [18] present the range of transmission and the channel capacity for intra-body systems for general healthcare applications. Again, Piro et al. [19] has studied the communication capabilities of a body area nano-network by carefully taking into account the inhomogeneous and disordered structure offered by biological tissues.

However, most of the works presented above consider the human tissue as a single level. In this work, a multi-layer communications method has been proposed. In addition, the reflection properties between blood, fat and skin are investigated. This work also calculates the propagation of electromagnetic waves inside the human tissue containing blood, skin and fat for single and multi-layers according to nano-sensor transmit power calculation. Transmit power calculation is an innovative topic which has not been investigated in detail before as it is in this paper. Hence, this work investigates Intra-Body Nano-Network communication propagation channel characteristics which are calculated using a theoretical approach that is modeled providing an evaluation about the losses, capacity, BER and SNR considering the multipath effect of the channel according to the nano-sensor transmit power calculation.

3 Model for Intra-Body Nano-Networks for Single and Multi-layers

The Friis Transmission Equation is used to calculate received power from an antenna to another antenna at some distance given a transmission frequency and antenna gains. Friis Equation is used to find the ideal power received at an antenna from basic information about the transmission [20]. For the propagation in human tissue, noise power (NP), thermal noise and additional losses (L_{medium}) at the receiver which are caused by blood, skin and fat are added to Friis equation in formula (1). To calculate the NP, the Bandwidth (B) and ambient temperature (T), which is taken as body temperature of 310.15 K, need to be calculated. Consequently, the received signal in the Friis equation can be updated as [21]:

$$P_r(dBm) = P_t(dBm) + G_r(dB) + G_t(dB) \underbrace{-L_{FSPL}(dB) - L_{NP}(dBm) - L_{medium}(dB)}_{System\ Loss} \quad (1)$$

Table 1 shows the values in equations.

In Eq. (1) L_{NP} calculated as $10log_{10}(10^3 \times k_B \times T \times B)$. L_{medium} equals to:

$$L_{medium}(dB) = L_\beta + L_\alpha \quad (2)$$

L_{medium} (2) is a combination of L_β and L_α. L_α which is 8.96αd(dB) is the transmission loss caused by attenuation with attenuation constant α. L_β is the attenuation loss due to the difference of the wavelength of the signal in medium, λ, compared to the wavelength in free space, λ_0. So L_β can be also written as $20log(\lambda_0/\lambda)$. *Here, in this formula* $\lambda = 2\pi/\beta$ *and*

Table 1 Constants and parameters

Symbol	Quantity	Units	Symbol	Quantity	Units
P_r	Receiving antenna's power	dBm	α	Attenuation constant	1/m
P_t	Transmitting antenna's power	dBm	β	Phase shifting constant	rad/m
G_t	Transmitting antenna gain	dB	d	Distance between nano-sensors	m
G_r	Receiving antenna gain	dB	P_t	Transmit power	dBm
L_{FSPL}	Free space path loss	dB	L_f	Total path loss	dBm
c	Speed of ligh	m/s	P_n	Noise energy	dBm
L_{NP}	Receiver's noise power	dBm	L_{NP}	Noise power	dBm
B	Bandwidth	Hz	C	Capacity	bits/s
k	Boltzmann constant	j/K	Γ	Amplitude of the reflection coefficient	–
T	Ambient temperature	310.15 K	ϕ	Phase angle of the reflection coefficient	–
L_β	Attenuation loss	dB	α	Attenuation constant	–
L_α	Transmission loss	dB	X_1, X_2	Single and multi path channel model independent Rayleigh distributed random variables envelope	–

$\lambda_0 = c/f$ (Here c is speed of light) then L_β can be written as $154 - 20log(f) + 20log(\beta)$ *as dB.* Then L_{medium} which is our body in this work becomes:

$$L_{medium}(dB) = 6.4 + 20\log(d) + 20\log(\beta) + 8.69\alpha d$$
$$\alpha = 2\pi f\sqrt{\frac{\mu \in'}{2}\left[1 + (\frac{\in''}{\in'})^2 - 1\right]}, \beta = 2\pi f\sqrt{\frac{\mu \in'}{2}\left[1 + (\frac{\in''}{\in'})^2 + 1\right]} \tag{3}$$

where parameters and constants are also given in Table 1. Note that L_{medium} in (2) depends on the β, α of the human body [19]. The human body's dielectric properties in this paper are obtained from [14].

In these analyzes, the communication channel is modeled as an independent Rayleigh distributed random variable, *Xi,* $i \in \{1,2\}$ [22, 23]. The single-path model received energy spectral density is given by (4) and has a distribution of (5).

$$r = X^2 SNR \tag{4}$$

$$f(r) = \frac{1}{E\left[X_1^2\right]SNR}\exp\left(\frac{E\left[X_1^2\right]SNR}{E\left[X_2^2\right]SNR}\right) \tag{5}$$

The received signal is modeled as the addition of two independent Rayleigh distributed random variables.

Consequently, the composite attenuation constant, *X*, for the multi-path model is given by [22, 23]:

$$X^2 = X_1^2 + \left(X_2 \cdot \Gamma \cdot \exp\left(-\alpha\Delta(r)\right)\right)^2 - 2 \cdot X_1 \cdot X_2 \cdot \Gamma \cdot \exp\left(-\alpha\Delta(r)\right) \times \cos\left(\pi - \left(\phi - \frac{2\pi}{\lambda}\Delta(r)\right)\right) \tag{6}$$

The SNR is given by $SNR = P_t - L_f - P_n$ in paper [21]. In this paper P_t assumes -15 to 5 dBm which are low enough for nano-node [7]. L_{NP} is given by (7) as dBm [24]:

$$L_{NP} = 10log_{10}(1000 \times k \times T \times B)(dBm) \tag{7}$$

According to paper [23] 2PSK modulation has more range when we compare with other modulations. For this reason, in this paper 2PSK modulation is considered. The BER rate for 2 PSK is $0.5erfc((SNR)^{1/2})$ in additive white Gaussian noise (AWGN) [23].

The multi-path channel model in blood, fat and skin is shown in Fig. 2. The reflections are the same in the other human tissue because according to the papers [25, 26] the relative magnetic permeability is 1 in all parts of the body. The single path is the direct path, which is shown with the red line between the two sensors in Fig. 2. The medium all around the sensor nodes can be considered homogeneous for instance the model is suitable for higher depths.

The multi-path channel model is given by (8) [20, 21, 25]

$$\begin{aligned} &L_f(dB) = L_{Human\ Tissue}(dB) - 10\log\sqrt{A} \\ &A = 1 + (\Gamma \times \exp(-\alpha\Delta r))^2 - 2\Gamma\exp(-\alpha\Delta r)^2 \times \cos\left(\pi - \left(\phi - \frac{2\pi f}{\lambda}\Delta(2)\right)\right) \\ &\Delta r = r - d, r = r1 + r2\ (in\ Fig.\ 2) \end{aligned} \tag{8}$$

where human tissue is the path loss due to the single path given in (4) and the second part of the equation is the second path's attenuation factor which is unit in dB [22, 23, 27].

$$C = B\log_2\left[1 + S/N\right] \tag{9}$$

Capacity is the highest data rate that can be delivered reliably over a channel. The resulting capacity is measured in bits/s because the logarithm is taken in base 2 in Eq. (9) [14]. The unit of the bandwidth of the channel (B) is hertz. The signal and noise powers are S and N. The ratio between S and N is called SNR. The detailed model of the system is shown step by step in Fig. 3 to make this section more easily readable.

4 Numerical Results

In this part the proposed channel model's path loss, BER, attenuation factor, channel capacity and SNR values are given.

Figure 4a gives the values of path loss for blood, skin and fat. Figure 4b gives a 3D version of Fig. 4a. In Fig. 4a and in the following figures the red lines show the blood, the black lines show the skin and the blue lines show the fat. The lines style at figures are the same in the following figures that is why lines style legend is not given in some following figures not to make them complicated. Figure 4 shows that when the frequency and distance increases path loss is increased. Path loss is directly proportional to frequency and distance. Figure 4 also shows that blood has higher path loss than skin and fat. The reason why the blood has the highest path loss is that the amount of water in blood is more than in skin and fat. The human blood contains about 45% of erythrocytes and 54.3% of plasma by volume. The plasma contains about 92% water, while the erythrocytes, about 64% by weight. These papers [28–30] also prove why the water has higher absorption and path loss.

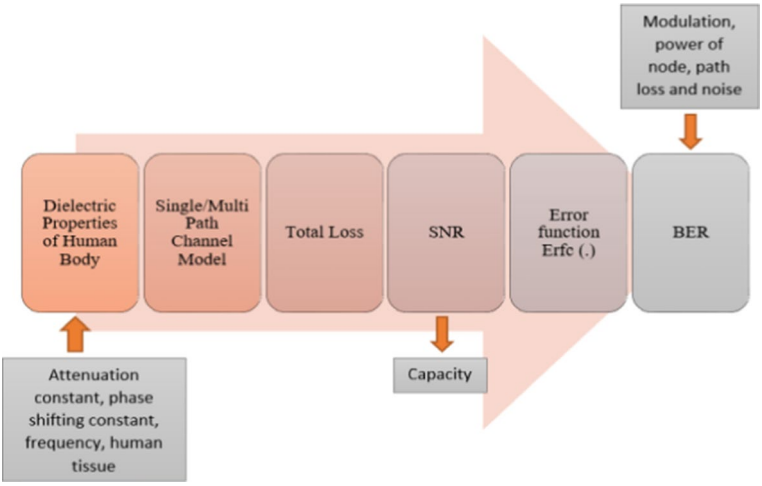

Fig. 3 Detailed model of the system

Figure 5a shows BER vs. distance for 0.5–1.5 THz. Figure 5b examines the BER for blood in the case of − 15 to 5 dBm transmit power and frequency at 0.5 THz. The results show that BER of the 0.5–1.5 THz operating frequencies in blood, skin and fat for the single path channel model increases between 1 and 3 mm for blood, 1–5 mm for skin and 2–7 mm for fat at minimum received signal power of − 5 dBm. The millimeter size communication distance increments are very important for nano-nodes inside the body. Figure 5 proves that the communication range depends on the value of the dielectric loss of the human body, remaining power of the node and the operating frequency. In Fig. 5b shows that each 5 dBm increment in P_t increases the communication distance around 0.1 mm. Figure 5c, d gives the values of capacity and SNR respectively that have been calculated from (8). Figure 5c shows that path loss increments cause less capacity and Fig. 5d shows that when the frequency decreases SNR increases and when the path loss increases SNR decreases that is why 0.5 THz fat has the highest SNR.

Figure 6a, b give the values of path loss at 0.5–1.5 THz for multi-path channel according to distance and depth respectively. When we compare Fig. 6a with Fig. 4a the path loss is around 80–300 dB in one-path model and the path loss is around 100–300 dB in multi-path model. Figure 6a also shows that in the multi-path model, communication distance at path loss 100 dB is up to 0.8 mm, 1.4 mm and 2 mm in blood, skin and fat respectively. Also in one-path model, the range is increased by 0.2 mm, 0.4 mm and 0.6 mm in blood, skin and fat respectively at 0.5 THz. Added reflection component of the signals do not help to increase the communication distance in the multi-path model because there is not much reflection in human tissue as seen in Fig. 6b. Figure 6b also shows that path loss values depend on human tissue distance and depth. Fluctuations at Fig. 6b decreases when the depth increases and almost disappears after distance around 0.2 mm. Figure 6c shows path loss, distance and depth relation in 3D dimensions at 0.5 THz. The 3D graph shows that at depths smaller than 0.2 mm there is a wave, which is too small to affect communication distance. In Fig. 6d attenuation factor is given which is the second part of the Eq. 7. As seen in the Fig. 6d attenuation factor decreases at depths smaller than 0.2 mm this caused the increased path loss in multi-path model and decreased the communication distance.

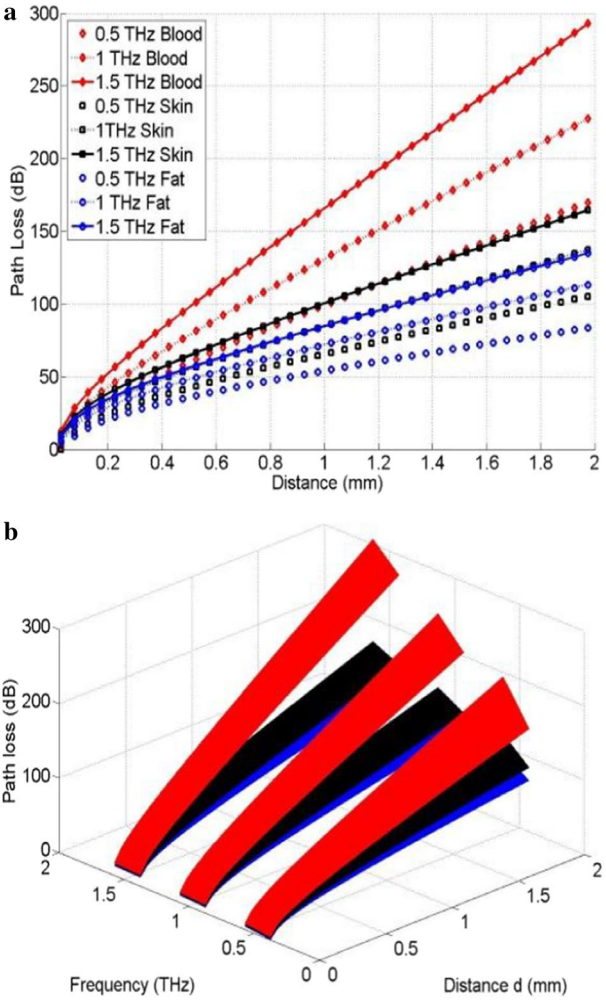

Fig. 4 Path loss vs. distance for 0.5 to 1.5THz in single-path channel model. **a** 2D version, **b** 3D version

This is also one reason why the multi-path channel model has smaller communication distance than one path-channel model.

Figure 7 shows BER vs. distance for 0.5–1.5 THz operating frequencies for the multi-path channel model. BER versus depth has not been given because there is almost zero BER at all depths. Figure 7a shows that the increment in the path loss has small effect on BER in multi-path channel model. The BER rate is directly proportional to the distance. Figure 7b examines the BER for blood in the case of − 15 to 5 dBm transmit power P_t at frequency 0.5–1.5 THz. When we compare Figs. 5b with 7b we see that there is no much difference between one-path and multi-path channel models. Only in the multi-path channel model, the transmission distance decreases around 1 mm at 0.5 THz.

Figure 8 shows Capacity versus distance and depth for 0.5–1.5 THz operating frequencies for the multi-path channel model. Figure 8a gives capacity values according to the distance at − 5 dBm transmit power. Figure 8b gives capacity values according to depth at − 5 dBm transmit power. Figure 8c gives capacity values according to distance at − 15

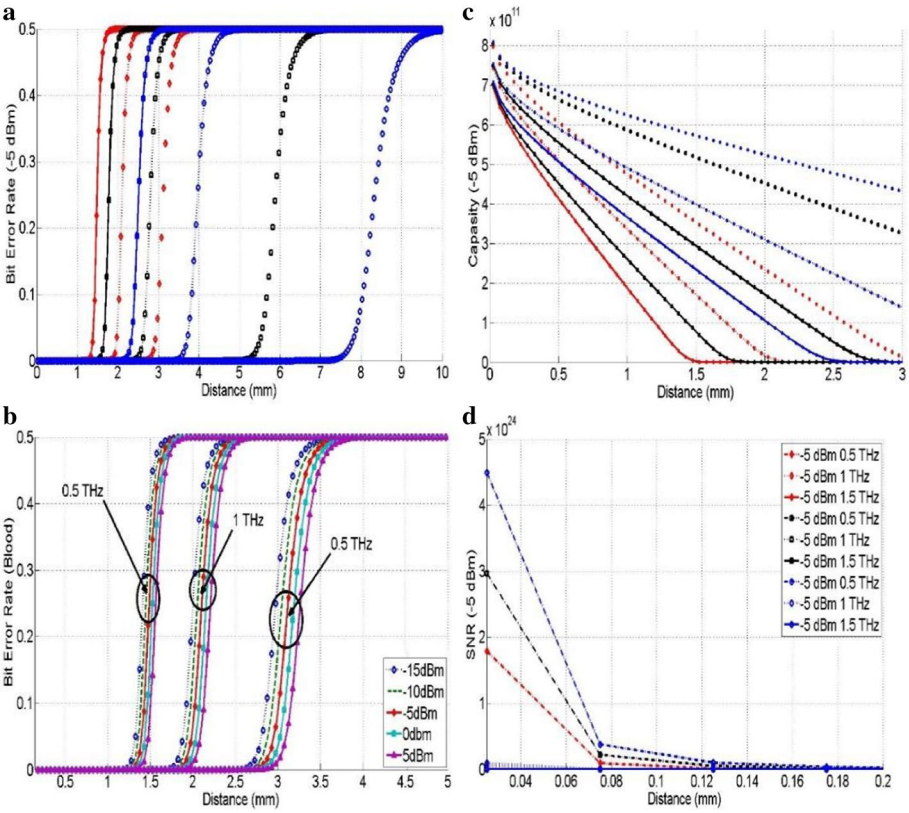

Fig. 5 BER, capacity and SNR versus distance for 0.5 to 1.5THz in single-path channel model. **a** BER versus distance, **b** BER for blood, **c** capacity, **d** SNR

to 5 dBm from 0.5 to 1.5 THz. From Fig. 8a we can understand that capacity and path loss inversely proportional to each other as expected. Figure 8b shows the capacity at − 5 dBm transmit power according to depth. Fluctuations at Fig. 8b decreases when the depth increases and almost disappears after distance around 0.2 mm as in the Fig. 6b. Figure 8c gives capacity values according to distance at − 15 to 5 dBm transmit power in the blood. Figure 8c also shows that frequency and capacity inversely proportional to each other and transmit power increases the capacity as expected.

Figure 9 shows SNR vs. distance and depth for 0.5–1.5 THz operating frequencies for the multi-path channel model. Figure 8a gives SNR values according to distance at − 5 dBm transmit power. Figure 8b gives SNR values according to depth at − 5 dBm transmit power. Figure 8c gives SNR values according to distance at − 15 to 5 dBm from 0.5 to 1.5 THz. From Fig. 9a we can understand that SNR and path loss are inversely proportional to each other as expected. Figure 9b shows the SNR at − 5 dBm transmit power according to depth. Fluctuations at Fig. 8b decreases when the depth increases and almost disappears after distance around 0.4 mm but see the effect at capacity and path loss up to 0.2 mm. Figure 9c gives SNR values according to distance at − 15 to 5 dBm transmit power. Figure 9c also shows that frequency and SNR inversely proportional to each other and transmit power increases the capacity as expected. At Fig. 9c SNR values of 1 THz and 1.5

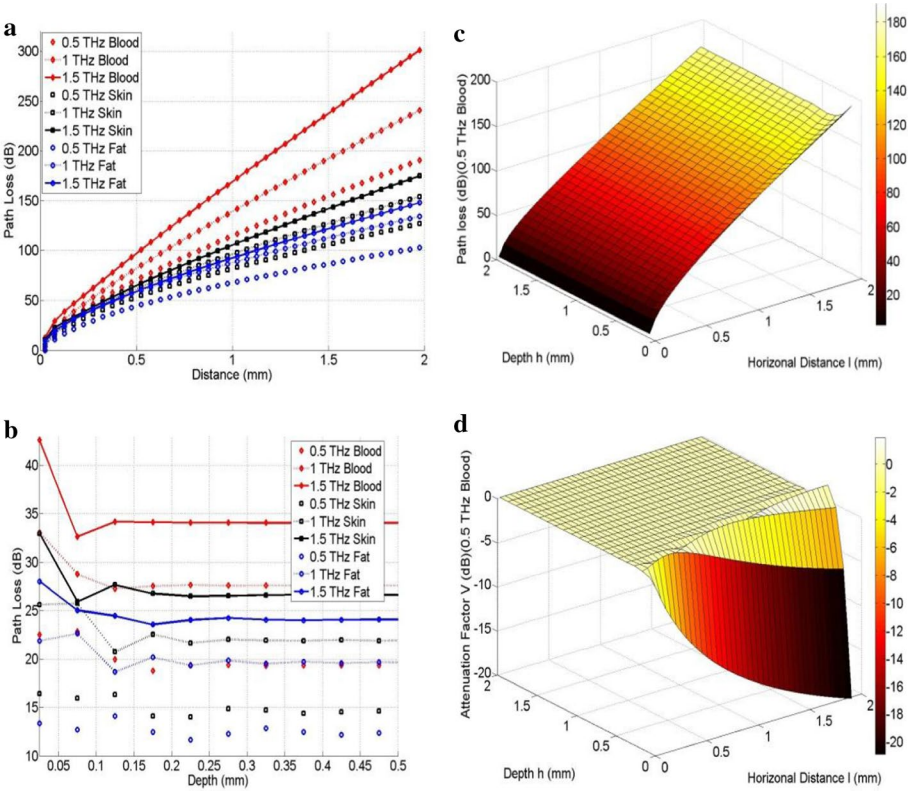

Fig. 6 Path loss vs. distance and depth for 0.5–1.5THz in multi-path channel model. **a** Path loss versus distance, **b** Path loss versus depth. **c** Path Loss, Distance and Depth Relation. **d** Attenuation

THz frequencies are not given because they are around the zero level. SNR values can help other researchers who are working on terahertz intra body networks. SNR is also affected from distance, frequency depth and transmit power. Figure 9 also reminds us that SNR is indirect proportional to frequency and direct proportional to transmit power.

5 Conclusion

Due to the small communication range inside the human body EM waves do not propagate easily especially in THz Bands. This paper examines the path loss, BER, channel capacity and SNR of nano-sensors propagating THz EM waves inside the blood, skin and fat according to transmit power and channel type. Briefly, the paper sets the theoretical background for the propagation of THz EM waves in blood, skin and fat in the THz range and determines the incurred path loss, BER, capacity and SNR of nano-sensors in single-channel and multi-channel. The paper also shows the reasons for why the multi-path channel model has smaller communication distance than one path-channel model. Numerical evaluations show that data communication is possible over the 0.01–1.5 THz band at transmit power − 15 to 5 dBm but to reach more communication distance, a new communication

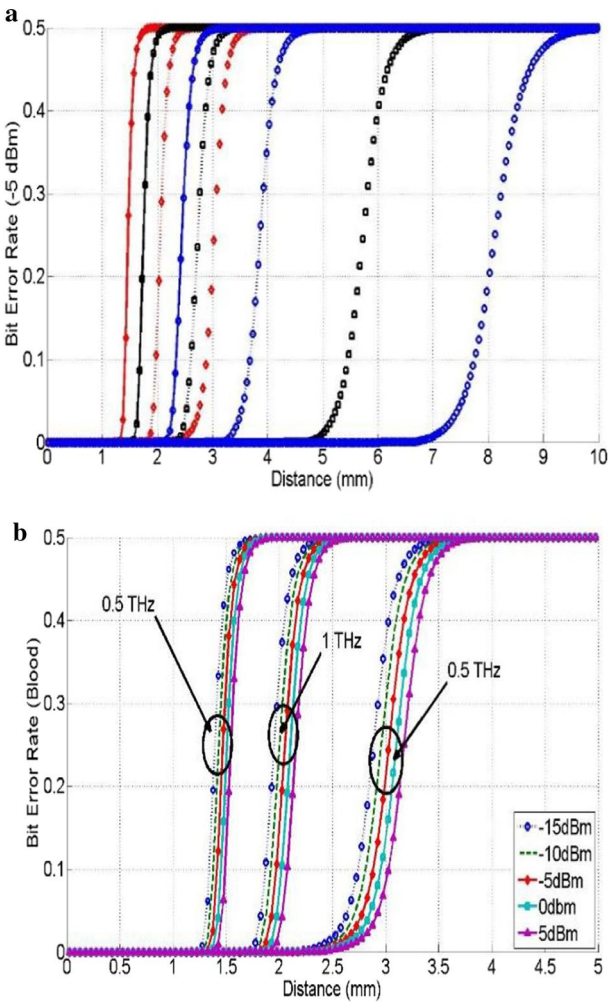

Fig. 7 BER versus distance for 0.5–1.5THz in multi-path channel model. **a** BER versus distance, **b** BER for blood

model needs to be investigated. Theoretical results show that wireless nano-sensor can communicate through the human body but thermal noise is too high to use the THz waves inside the human body. That is why new techniques need to be develop not to harm the body at THz range. The results in this paper also aim to guide other researchers that will be working in the area of the intra-body nano-networks. In the future, experiments can be done by using spectroscopy at THz range to validate the numerical findings.

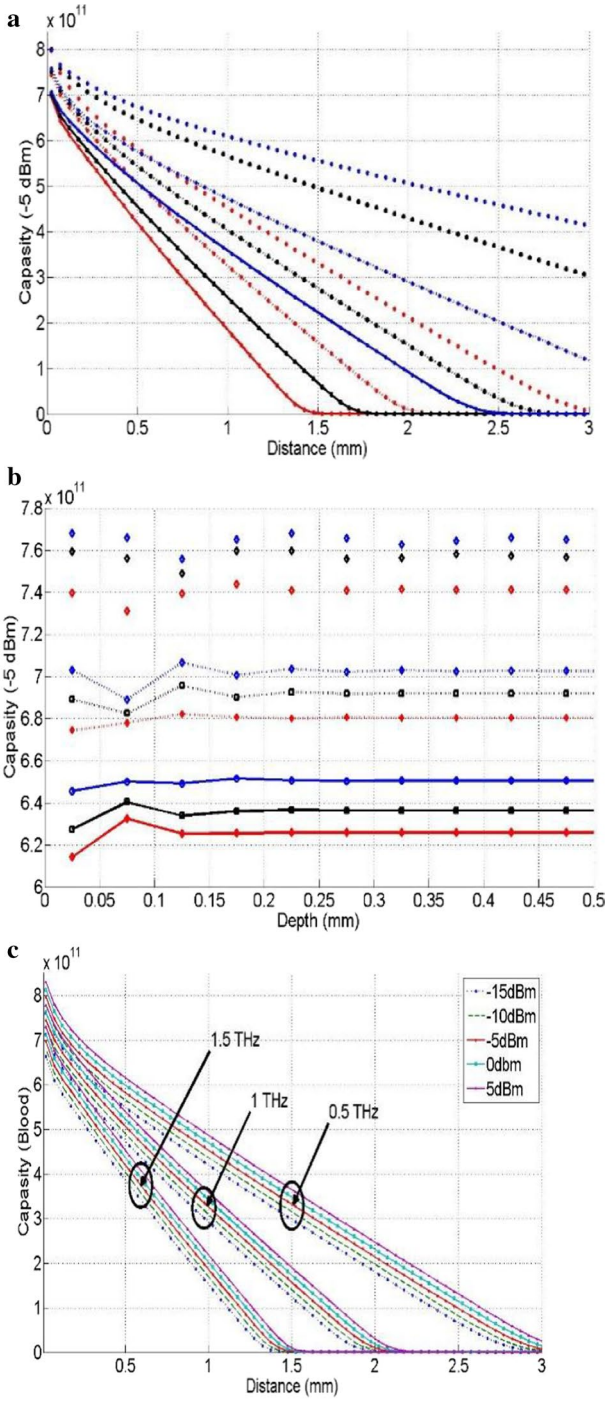

Fig. 8 Capacity vs. distance and depth for 0.5 to 1.5THz in multi-path channel model. **a** Capacity versus distance. **b** Capacity versus depth. **c** Capacity in the Blood

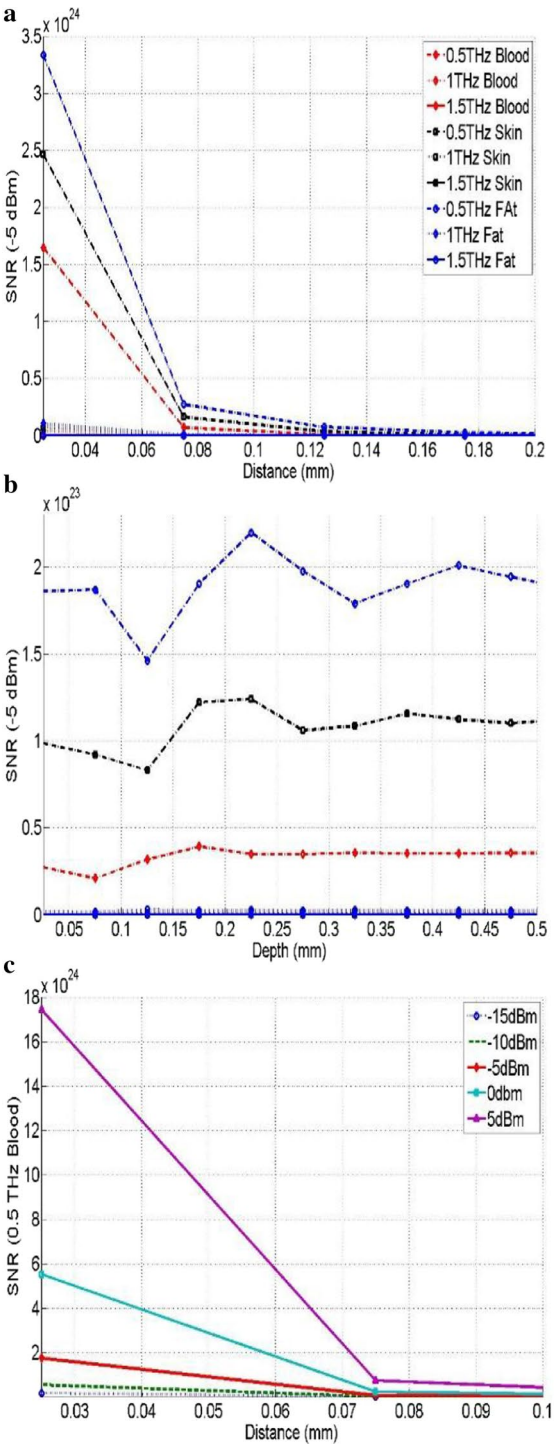

Fig. 9 SNR versus distance and depth for 0.5 to 1.5THz in multi-path channel model. **a** SNR versus distance. **b** SNR versus depth. **c** SNR in the Blood

References

1. Akyildiz, I. F., & Jornet, J. M. (2010). Electromagnetic wireless nanosensor networks. *Nano Communication Networks, 1*(1), 3–19.
2. Akyildiz, I. F., Brunetti, F., & Blázquez, C. (2008). Nanonetworks: A new communication paradigm. *Computer Networks, 52*(12), 2260–2279.
3. Chopra, N., et al. (2014). Understanding and characterizing nanonetworks for healthcare monitoring applications. In *2014 IEEE MTT-S international microwave workshop series on RF and wireless technologies for biomedical and healthcare applications (IMWS-Bio)*. IEEE.
4. Feynman, R. P. (1992). There's plenty of room at the bottom [data storage]. *Journal of Microelectromechanical Systems, 1*(1), 60–66.
5. Abdelaziz, A. F., et al. (2015) Terahertz signal propagation analysis inside the human skin. In *2015 IEEE 11th International Conference on Wireless and Mobile Computing, Networking and Communications (WiMob)*. IEEE.
6. Bush, S. F. (2010). *Nanoscale Communication Networks*. Norwood: Artech House.
7. Dressler, F., & Fischer, S. (2015). Connecting in-body nano communication with body area networks: Challenges and opportunities of the Internet of Nano Things. *Nano Communication Networks, 6*(2), 29–38.
8. Singh, S. P., Singh, S., Guo, W., Mishra, S., & Kumar, S. (2020). Radiation absorption noise for molecular information transfer. *IEEE Access, 8,* 6379–6387.
9. Pierobon, M., & Akyildiz, I. F. (2010). A physical end-to-end model for molecular communication in nanonetworks. *IEEE Journal on Selected Areas in Communications, 28*(4), 602–611.
10. Lee, S. J., et al. (2015). Design of wireless nanosensor networks for intrabody application. *International Journal of Distributed Sensor Networks, 2015,* 90.
11. Akkaş, M. A. (2016). A comparative review of mote size and communication method for wireless sensor network. In *Applied mechanics and materials* (Vol. 850). Trans Tech Publications.
12. Akkaş, M. A. (2016). Nano-sensor capacity and SNR calculation according to transmit power estimation for body-centric nano-communications. In *2016 3rd international symposium on wireless systems within the conferences on intelligent data acquisition and advanced computing systems (IDAACS-SWS)*. IEEE.
13. Akyildiz, I. F., Jornet, J. M., & Pierobon, M. (2011). Nanonetworks: A new frontier in communications. *Communications of the ACM, 54*(11), 84–89.
14. Yang, K., et al. (2015). Numerical analysis and characterization of THz propagation channel for body-centric nano-communications. *IEEE Transactions on Terahertz Science and Technology, 5*(3), 419–426.
15. Singh, S. P., Kumar, A., & Kumar, S. (2017). Novel expressions for CEP/BEP under GGD noise for nano communication system. *International Journal of Electronics Letters, 5*(4), 463–474.
16. Elayan, H., Johari, P., Shubair, R. M., & Jornet, J. M. (2017). 'Photothermal modeling and analysis of intrabody terahertz nanoscale communication. *IEEE Transactions on NanoBioscience, 16*(8), 755–763.
17. Zhang, R., Yang, K., Abbasi, Q. H., Qaraqe, K. A., & Alomainy, A. (2018). Analytical modelling of the effect of noise on the terahertz in-vivo communication channel for body-centric nano-networks. *Nano Communication Networks, 15,* 59–68.
18. Piro, G., et al. (2015). Terahertz communications in human tissues at the nano-scale for healthcare applications. *IEEE Transactions on Nanotechnology, 14*(3), 404–406.
19. Piro, G., et al. (2016). Terahertz electromagnetic field propagation in human tissues: A study on communication capabilities. *Nano Communication Networks, 10,* 51–59.

20. Friis, H. T. (1946). A note on a simple transmission formula. *Proceedings of IRE, 34,* 254–256. https://doi.org/10.1109/jrproc.
21. Akkaş, M. A. (2018). Using wireless underground sensor networks for mine and miner safety. *Wireless Networks, 24,* 1–10.
22. Vuran, M. C., & Silva, A. R. (2010) Communication through soil in wireless underground sensor networks–theory and practice. In *Sensor networks* (309–347). Berlin: Springer.
23. Akyildiz, I. F., Sun, Z., & Vuran, M. C. (2009). Signal propagation techniques for wireless underground communication networks. *Physical Communication, 2*(3), 167–183.
24. Couch, I. I., & Leon, W. (1994). *Modern communication systems: Principles and applications*. Upper Saddle River: Prentice Hall.
25. Pethig, R., & Kell, D. B. (1987). The passive electrical properties of biological systems: Their significance in physiology, biophysics and biotechnology. *Physics in Medicine and Biology, 32*(8), 933.
26. Collins, C. M., et al. (2002). Numerical calculations of the static magnetic field in three-dimensional multi-tissue models of the human head. *Magnetic Resonance Imaging, 20*(5), 413–424.
27. Li, L., Vuran, M.C., & Akyildiz, I. F. (2007). Characteristics of underground channel for wireless underground sensor networks. In *Proceedings of Med-Hoc-Net'07*.
28. Akkaş, M. A., & Sokullu, R. (2015). Channel modeling and analysis for wireless underground sensor networks in water medium using electromagnetic waves in the 300–700 MHz range. *Wireless Personal Communications, 84*(2), 1449–1468.
29. Akkaş, M. A., Akyildiz, I. F., & Sokullu, R. (2012). Terahertz channel modeling of underground sensor networks in oil reservoirs. In *Global communications conference (GLOBECOM), 2012 IEEE*. IEEE.
30. Akkaş, M. A. (2019). Terahertz wireless data communication. *Wireless Networks, 25,* 1–11.

Mustafa Alper Akkaş received his B.S. degree in Electrical and Electronics Engineering from Erciyes University in 2006. He received his Ph.D. degree in the Department of Electrical Engineering and Electronics at Ege University in 2014. Currently, he is an associate professor at the Department of Computer Engineering at Bolu Abant Izzet Baysal University. His research interests include Wireless underground communication networks, Terahertz-band communication networks, Intra-body wireless nanosensor networks and Internet of Things. He was a visiting student at Georgia Institute of Technology, in the Broadband Wireless Networking Lab under the supervision of Prof. Ian F. Akyildiz from September 2011 to May 2012.